Fine-scale whisker growth measurements can reveal temporal foraging patterns from stable isotope signatures

Roxanne S. Beltran[1,4,*], Megan Connolly Sadou[2], Richard Condit[3], Sarah H. Peterson[1], Colleen Reichmuth[2], Daniel P. Costa[1]

[1]Department of Ecology & Evolutionary Biology, University of California, Santa Cruz, CA 95060, USA
[2]Institute of Marine Sciences, Long Marine Laboratory, Santa Cruz, CA 95060, USA
[3]Smithsonian Tropical Research Institute, Balboa, Panama City, 0843-03092, Panama

[4]*Present address:* Department of Biological Sciences, University of Alaska, Anchorage, AK 99508, USA

ABSTRACT: Stable isotope analysis of slow-growing, metabolically inert tissues is a common method for investigating foraging ecology in migratory animals, as direct observations of feeding are often not possible. Using tissue growth dynamics to interpret foraging timelines can maximize the utility of foraging data; however, applying inappropriate growth models is problematic, and high-resolution growth measurements are seldom made. We used photogrammetry to repeatedly measure the length of whiskers in 93 follicles over 670 d in a trained, captive northern elephant seal *Mirounga angustirostris*. We developed and optimized a follicle-specific growth model to describe the 18 000 whisker length measurements. Whiskers from the captive seal exhibited asymptotic growth that was described by the von Bertalanffy growth function. Applying the growth model to serially sampled whiskers from 4 free-ranging adult female northern elephant seals resulted in alignment of peaks in δ^{15}N along the length of whiskers with the breeding haul-out period, when seals are not feeding. Our study provides a high-resolution whisker growth model and is the first to use whisker growth dynamics to improve temporal interpretation of isotopic ratios.

KEY WORDS: Vibrissae · Whisker · Asymptotic growth rate · Stable isotope · Seal

INTRODUCTION

Analysis of stable carbon (δ^{13}C) and nitrogen (δ^{15}N) isotope values in animal tissues can supplement or replace traditional methods for describing the diet of highly mobile, far ranging animals (Newsome et al. 2012). Time-depth recorders, accelerometers, stomach temperature sensors, animal-mounted cameras and other instruments have been used to provide insight into foraging behavior of marine animals (Le Boeuf et al. 2000, Bradshaw et al. 2003, 2004, Kuhn et al. 2009, Thums et al. 2011, Costa 2012, Naito et al. 2013); however, the dietary composition of many species remains poorly understood due to the inherent limitations of those tools.

Isotopic measurements of different tissues collected from an individual animal can reveal dietary information on varying temporal scales, because different tissue types have characteristic metabolic (i.e. turnover) rates (Hobson & Clark 1992, Ogden et al. 2004, MacNeil et al. 2005, MacAvoy et al. 2006, Logan & Lutcavage 2010, Newsome et al. 2012). Continuously growing whiskers can produce a sequential record of dietary information over large temporal scales, thus offering an advantage over integrated tissues with faster turnover rates such as blood (Gannes et al. 1998, Dalerum & Angerbjörn 2005, Newsome et al. 2010). Time series isotope data obtained from whiskers can address important ecological questions that point samples cannot (Zhao & Schell 2004),

including within-individual variation (Newsome et al. 2009, Hückstädt et al. 2012a,b), seasonal diet patterns (Lee et al. 2005, Newland et al. 2011), individual foraging strategies (Lewis et al. 2006), changes in habitat utilization (Bearhop et al. 2003, Cherel et al. 2009), and behavioral responses to perturbations (Bodey et al. 2010). Further, the use of whiskers in stable isotope analyses for mammals allows for nonlethal, minimally invasive tissue sampling (Newsome et al. 2010, Hückstädt 2012, Tyrrell et al. 2013). Researchers have used whisker analyses to infer tissue deposition time by identifying cycles in isotopes (Cherel et al. 2009, Newland et al. 2011) or biomarkers (Robertson et al. 2013) that could reflect changes in foraging behavior, but to our knowledge, no one has applied fine-scale whisker growth rates to interpret stable isotope data.

Species-specific whisker growth models are required in order to assign realistic time-scales to isotopic information embedded in whiskers. Unfortunately, whisker growth and shedding studies are limited to a small number of mammals, and inconsistencies in reported growth values have yet to reveal a universal set of growth parameters (Oliver 1966, Hirons et al. 2001, Greaves et al. 2004, Zhao & Schell 2004, Newland et al. 2011, Robertson et al. 2013). Recent photogrammetric and isotopic studies suggest that some species exhibit linear whisker growth (Hirons et al. 2001, Tyrrell et al. 2013), while the von Bertalanffy organic growth equation best describes asymptotic whisker growth in other species (Greaves et al. 2004, Hall-Aspland et al. 2005).

Previous studies have found whisker shedding and growth patterns to be independent of the relatively rapid pelage molt in some species (Ling 1968, Greaves et al. 2004), which suggests that animals maximize function of the vibrotactile sensory system by ensuring that a proportion of whiskers are at their asymptotic length at any given time (Hirons et al. 2001, Greaves et al. 2004). In addition, asymptotic whisker lengths are strongly associated with row position across the mystacial cheek pads in rats, mice, and seals, such that whisker length increases predictably from rostral to caudal sides in any row (Brecht et al. 1997). In this way, individuals can retain a flattened sensory plane despite the curvature of the muzzle.

To obtain high-resolution growth data across an entire whisker bed, we consistently measured growth of whiskers in a captive northern elephant seal *Mirounga angustirostris* using validated photogrammetric methods and found that a von Bertalanffy growth model best fit the data. We applied the values ob-

tained from the model to predict the time periods during which segments of whisker tissues are established in wild elephant seals. With the appropriate uncertainty considered, we demonstrate how temporal information can be applied to foraging data with relatively high confidence. When applied to stable isotope analysis results, whisker growth rates refine current methods for dietary reconstruction in mammals.

MATERIALS AND METHODS

Whisker measurement

The main subject of this study was an adult (16 yr old) female northern elephant seal called Burnyce (National Marine Fisheries Service ID no. NOA000 4829). The seal was housed at Long Marine Laboratory at the University of California Santa Cruz from 1994 to 2011. Following the procedure described in Connolly Sadou et al. (2014), we obtained 3 photographs each of the right and left mystacial whiskers during weekly sessions spanning a period of 670 consecutive days (28 January 2009 to 29 November 2010). The seal was trained through positive reinforcement techniques to maintain steady contact with a PVC chin station (Fig. 1) for the duration of each session. All photographs were taken with a Kodak EasyShare Z650 digital camera (6.1 megapixel) at a distance of approximately 38 cm, a height of 30.5 cm and a 30° angle from the tip of the seal's nose. A 1 cm scaling bar was positioned in the frame

Fig. 1. *Mirounga angustirostris*. A captive northern elephant seal was trained to rest her chin at a station, with a scale bar (1 cm grid) placed perpendicular to the camera lens and resting above the last whisker of the apical mystacial row to allow measurements of whisker length

of each photograph parallel to the animal's muzzle at the position of the upper leftmost whisker (Fig. 1).

To ensure consistency in measurements, we evaluated photographs for 5 criteria: (1) focal length was consistent at 38 mm; (2) follicles were visible; (3) whisker tips were visible; (4) scaling bar was perpendicular to camera; and (5) whiskers were relaxed. If photographs did not meet all 5 criteria, they were excluded from analysis. The remaining photographs were calibrated to the scaling grid using Image Processing and Analysis in Java (ImageJ, NIH, http://rsb.info.nih.gov/ij). We identified individual whiskers throughout the study using the northern elephant seal bed map from Connolly Sadou et al. (2014). We analyzed over 18000 whisker length measurements from photographs taken during 52 sessions over the sampling period, allowing us to generate time-series measurements of whisker length for each follicle (available at http://dx.doi.org/10.5479/si.ctfs.0002). The right and left mystacial beds contained 48 and 45 follicles, respectively, and whiskers were distributed across 7 rows.

Whisker growth model

Based on our descriptive assessment of the data, which showed rapid growth followed by slowing at a certain asymptotic length, we started with the von Bertalanffy model described by:

$$L_t = L_\infty \cdot (1 - e^{-K(T-T_0)}) \tag{1}$$

where asymptotic length (L_∞), time of initial growth (T_0), and a curvature constant (K) predict the length (L) at time T (Sparre & Venema 1999). Growth is $K \times$ age at time T_0, then declines steadily toward 0. A high K value represents more rapid ascent to the asymptote. Solving for T provides an equation for the age (or deposition time) of a whisker at a given length:

$$T = \left[\frac{-1}{K} \cdot \ln\left(1 - \frac{L_T}{L_\infty}\right) \right] + T_0 \tag{2}$$

This simple model can be used to describe growth of a single whisker. However, the complete model describes sequential whiskers and shedding events at a single follicle. The model requires 4 parameters per whisker within a follicle: (1) initiation date (T_0 in Eq. 1); (2) growth parameter (K in Eq. 1); (3) asymptotic whisker size (L_∞ in Eq. 1); and (4) lifespan M, not included in the basic von Bertalanffy model but necessary to model a sequence of whiskers. A fully detailed model of 2 sequential whiskers would thus need 4 parameters for each whisker: $T_0^{(i)}$, $M^{(i)}$, $K^{(i)}$,

Table 1. *Mirounga angustirostris*. Modeled growth parameters from Eqs. (1) & (2) for whiskers of a captive northern elephant seal derived from photogrammetric whisker length measurements. K: curvature constant, where a high K represents a more rapid assent to asymptotic length; L_∞: estimated asymptotic length of each whisker; Lifespan: time between initial growth and shedding; Lag: time between shedding of one whisker and growth of a second whisker from a single follicle

Parameter	K (cm d^{-1})	L_∞ (cm)	Lifespan (d)	Lag (d)
Mean	0.0132	8.17	369.14	28.82
SD	0.0065	3.69	73.58	12.72
N	44	44	14	44
Min	0.0045	2	250	14
Max	0.0324	16.4	517	77

$L_\infty^{(i)}$ for the ith whisker. Because the data never included 3 complete whisker lifespans at one follicle, and only a few included 2, abbreviated models with fewer parameters were needed.

We were able to apply the abbreviated models to 44 out of 93 whisker follicles (Table 1). There were insufficient reliable follicle measurements on the others because of the short, thin nature of their whiskers, or because follicles remained empty throughout the study.

Three-whisker model

Of the 44 follicles we examined, 14 included observations of one whisker's entire lifespan, from initiation to shedding (Fig. 2a–c). In 10 of these follicles, one whisker was present at the start of the study and then shed, a second whisker initiated and shed, and a third whisker initiated and remained at the end of the study. In the other 4 follicles, no whisker was present at the onset, then a whisker grew and shed, and a third whisker started. The initiation date T_0 of the first whisker was not observed in any of these, and the lifespan M was only observed in 1 whisker. Moreover, the growth portion with curvature was always missing for the initial whisker, and in 11 of 14 follicles, it was largely missing for the third whisker, meaning only the second whisker provided data on the curvature constant K. We thus reduced the full 12 parameters to 8, because (1) we assumed K was the same for all whiskers ($K = K^{(1)} = K^{(2)} = K^{(3)}$); (2) we assumed 2 separate lifespans M, with the second and (if present) third whiskers sharing M while the first differed ($M^{(1)}$, $M^{(2)} = M^{(3)}$); (3) we likewise assumed 2 separate asymptotes, ($L_\infty^{(1)}$, $L_\infty^{(2)} = L_\infty^{(3)}$); and (4) we included all 3 initiation dates, $T_0^{(1)}$, $T_0^{(2)}$, $T_0^{(3)}$. We did
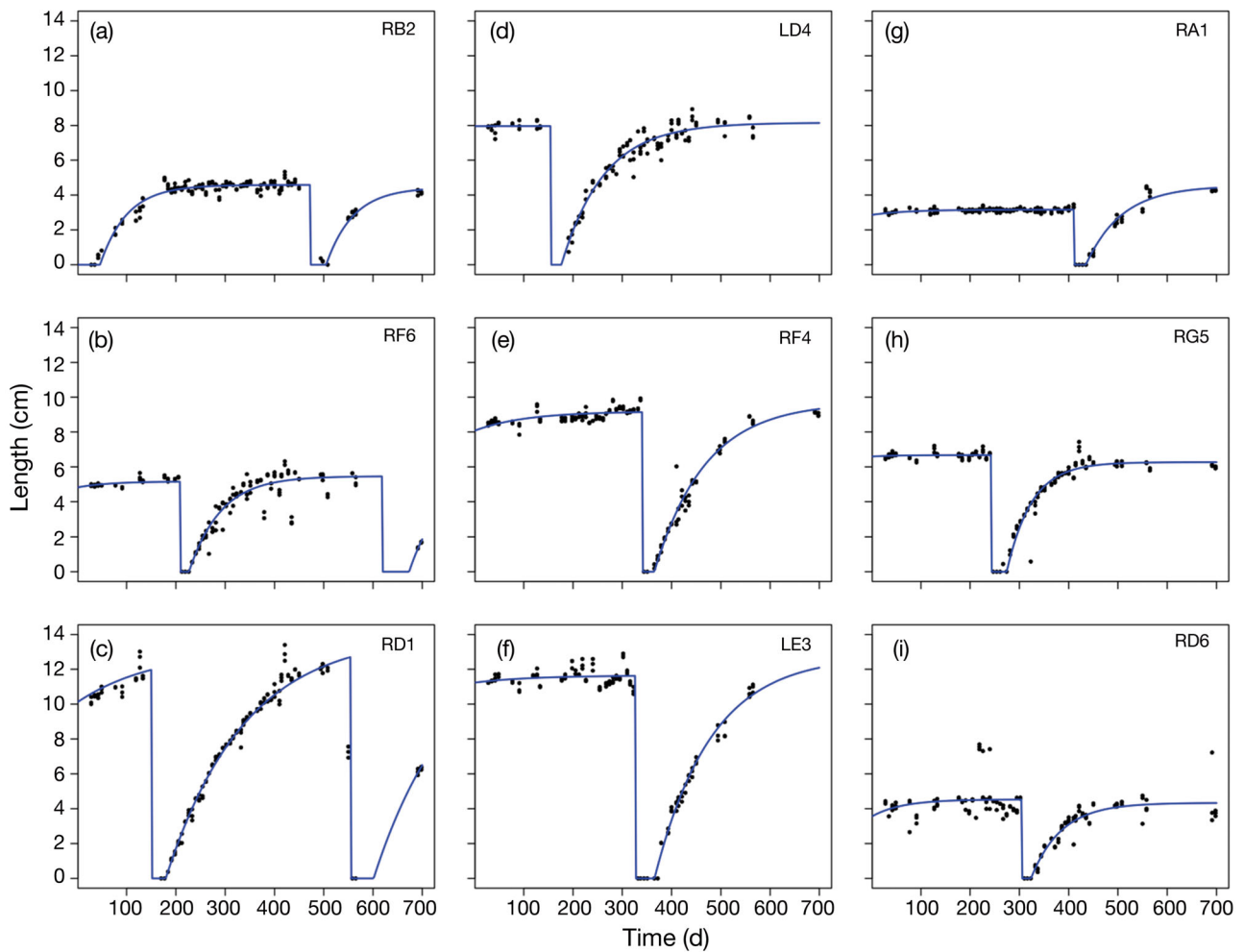
Fig. 2. *Mirounga angustirostris*. Representative time-series plots for vibrissal growth in a captive elephant seal. (a–c) Follicles (N = 14) that included observations of one whisker's entire lifespan from initiation to shedding, and (d–i) follicles (N = 30) that had 2 whiskers during the observations, but neither was observed for its full lifespan; after shedding of the first whisker, growth was rapid and non-linear. The code in the upper right of each plot indicates the bed (side of the snout; R: right, L: left), follicle row (A to G, from top to bottom of the snout), and follicle column (1 to 9) as described in Connolly Sadou et al. (2014). Black dots: raw photogrammetric measurements; blue line: growth model

not omit the first initiation date, because K was well-constrained by data for the second whisker, so that the first initiation date is in fact constrained by the curvature constant K and the shedding date. The 8 parameters in the 3-whisker model are thus $\theta = (K, M^{(1)}, M^{(2)}, L_\infty^{(1)}, L_\infty^{(2)}, T_0^{(1)}, T_0^{(2)}, T_0^{(3)})$.

Two-whisker model

Thirty other follicles had 2 whiskers during the observations, but neither whisker was fully observed over its lifecycle. One whisker was present at the outset and subsequently shed, and then a second whisker initiated and was still present at the end (Fig. 2d–i). Following the same logic for determining which parameters are well-constrained by the data, we built a 6-parameter model for these follicles: $\theta = (K, M, L_\infty^{(1)}, L_\infty^{(2)}, T_0^{(1)}, T_0^{(2)})$, with $K^{(1)} = K^{(2)} = K$ and $M^{(1)} = M^{(2)} = M$. The lifespan was necessary to build the model, but it was nearly unconstrained by the data and thus was excluded from subsequent data summaries. The $L_\infty^{(2)}$ was also poorly constrained, and we only used $L_\infty^{(1)}$ in data summaries.

Parameter fitting

Model parameters were estimated from data using a non-linear regression approach in a Bayesian

framework. This starts with a likelihood function defining the probability of observing one follicle's observations given a full set of whisker growth parameters. The likelihood requires an error model, which we assumed to be Gaussian with a standard deviation σ that increases linearly with whisker length:

$$\sigma = a + bL_{pred} \qquad (3)$$

where a and b are parameters, and L_{pred} is the model's prediction of whisker length. The parameters a and b must be estimated along with the growth parameters, 1 set for every follicle. A predicted whisker length (L_{pred}) was produced on each observation date T given the parameters:

$$L_{pred} = f(\theta, T) \qquad (4)$$

The likelihood of observed whisker length L, given modeled whisker length L_{pred} and parameters a, b, and σ from Eq. (3) was calculated as:

$$\text{Like}(L, \theta, a, b) = \text{Gauss}(L, \text{mean} = L_{pred}, \text{SD} = \sigma) \quad (5)$$

A standard way to locate best-fitting parameters for one set of data is to search for the parameters that maximize log(Like). We extended this with a Bayesian approach, thoroughly sampling parameter combinations close to the optimum to provide a best set of parameters plus credible intervals around them. This was accomplished by searching 7500 parameter combinations using a Metropolis algorithm to generate each new combination, discarding the first 2500 as burn-in (see Condit et al. 2007 for details). The resulting chain of 5000 estimates reproduces the posterior distribution for every parameter, and the mean of this distribution was taken as the single best estimate for a parameter. The 95th percentiles of the post burn-in chain were used as 95% credible intervals. The chain of parameters was also used to simulate whisker growth in a way that propagates all sources of error in the model. Source code in R for fitting the growth model is available along with a small subsample of data at http://dx.doi.org/10.5479/si.ctfs.0002.

Photogrammetric size versus true size

The observed and fitted whisker lengths from the equations above refer to photographic measurements, but Connolly Sadou et al. (2014) demonstrated by direct measurements of a subsample that photographs underestimate whisker size, mostly because direct measurements include a subdermal portion. Since the latter matters in isotope analysis, we applied a correction on top of the model of photographic length

(Eq. 4). First, we repeated Connolly Sadou et al.'s (2014) regression of direct vs. photographic size in the Bayesian framework to generate posterior distributions of the regression parameters c and d:

$$T = c + dL + \varepsilon \qquad (6)$$

where ε is a Gaussian error term, modeled exactly as in Eq. (3). The simulations then rely on draws from posterior distributions of model parameters θ plus c and d.

A simulation started with selection of 1 random set of von Bertalanffy growth parameters, θ, from the Bayesian posterior distributions. The model parameters needed to simulate 1 whisker's growth were curve K and asymptotic length L_∞. The parameter for initiation date was irrelevant, and lifespan was unnecessary as our interest was growth prior to the asymptote. We always chose both parameters from 1 whisker, in case K and L_∞ were correlated. The pair of parameters produced a single simulated trajectory of photographic size to full whisker size. Subsequent random draws from the same parameter distributions (same whisker) were used to produce 10 000 alternative growth curves and thus 95% credible intervals on the predicted photographic size of the whisker on any day. For each of those 10 000 curves, we utilized posterior distributions of the regression parameters in Eq. (6), randomly choosing 1 pair (c,d) to convert the photographic size to full whisker size. Each of the curves can be interpreted as 'length as a function of age' or 'age as a function of length'. From each curve, we used the age (in d) at 75% of the L_∞ to judge ages of whiskers that are still growing.

Whisker bed anatomy

To examine trends in length across the whisker bed, we examined L_∞ as a function of bed position for the captive seal. A prediction of $L_\infty \approx$ column + row + row^2 was regressed against the observed L_∞. We centered row and column by subtracting 4 from each. Source code in R for fitting the growth model is available at http://dx.doi.org/10.5479/si.ctfs.0002. Model fit was assessed using Akaike's Information Criterion (AIC; Hilborn & Mangel 1997).

Applications of whisker growth dynamics to dietary reconstruction of wild elephant seals

To apply the whisker growth dynamics to non-captive individuals, we obtained scaled muzzle pho-

tographs of 4 adult female northern elephant seals at the Año Nuevo elephant seal colony (San Mateo, California, USA; 37.108° N, 122.336° W), while seals were sedated for other procedures (Robinson et al. 2012) at the beginning of their catastrophic molt (May 2011). Photogrammetric lengths of all whiskers were determined using the same methods described for the captive study. We also plucked 1 whisker (including the subdermal component) from each of the 4 seals and recorded the whisker's bed location based on the standardized bed map provided in Connolly Sadou et al. (2014). These whiskers were most likely at L_∞ because their length was intermediate to the 2 adjacent whiskers on that row (Brecht et al. 1997). Whiskers were rinsed with de-ionized water and mild detergent to remove exogenous lipids and debris, washed with petroleum ether in an ultrasonic bath (Hassrick 2011), and measured for total length. On each whisker, only the 5 cm closest to the base were sampled, because growth rates estimated for phocid seals (mean ± SE: 0.10 ± 0.01 mm d^{-1}; Hall-Aspland et al. 2005) suggest that both the present molt and the prior breeding season for these seals would be contained within that part of the whisker. We divided the 5 cm section into ten 0.5 cm segments and discarded the segment closest to the base to avoid the influence of the subdermal $\delta^{15}N$ on overall values. Of the remaining 9 segments, we subsampled 0.5 ± 0.05 mg (mean ± SD) of whisker from the proximal end (i.e. closer to the base) and sealed each subsample in a tin boat. Samples were analyzed for $\delta^{15}N$ at the Light Stable Isotope Lab (University of California Santa Cruz) using a Carlo Erba elemental analyzer interfaced with a ThermoFinnigan Delta Plus XP mass spectrometer. Isotope ratios are expressed as δ values, which are reported in parts per thousand (‰) using: δX = 1000 × ($R_{sample} - R_{standard}$)/$R_{standard}$, where R_{sample} is the ratio of heavy to light isotopes (^{15}N:^{14}N), and $R_{standard}$ is the international reference standard. Since higher $\delta^{15}N$ values reflect catabolism during prolonged fasts (Lee et al. 2012), we expected peaks in $\delta^{15}N$ to align with the winter haul-out period (26 January to 9 March 2011) of the seals during the preceding breeding season. Sightings of the target individuals on land were recorded throughout the breeding season during a concurrent study (Robinson et al. 2012).

In addition to directly measuring the plucked whiskers, total length was predicted from follicle position by applying regression results from the captive seal. We also assigned an estimated age to each segment for which isotope ratios were measured, using the whisker growth rates derived from the captive seal. To do this, we calculated the whisker lifespan using simulations of whiskers whose asymptotes were similar. We then calculated T_0 by subtracting the lifespan from the date of whisker extraction. To examine the ability of post-hoc timestamps to correctly describe past life history events, we overlaid dated isotope ratios with the observed breeding haul-out periods for each free-ranging seal.

RESULTS

Whisker growth model

We obtained measurements in 52 out of the 66 weekly sampling sessions. Some measurements were missed due to poor animal motivation (no more than twice per 3 mo). Serial photogrammetric measurements of the captive elephant seal revealed rapid initial growth that slowed as whiskers reached an asymptote of 2.0 to 16.4 cm (Table 1). Whiskers of all sizes had similar initial growth, but small whiskers stopped growing sooner (Fig. 3). The mean (±SD) of the curvature constant K was 0.0132 (±0.0065). The mean (±SD) whisker lifespan was 369 (±74) d. Lifespan values were underestimated because the growth cycle of long-lived whiskers was less likely to be fully observed. Shedding was not coincident with the molt but was instead distributed throughout the year. There was a mean (±SD) of 28.8 (±12.7) d between the shedding of one whisker and the detection of a new whisker in photographs, which approximates the time required to re-grow the follicle. Without knowing whether a given whisker had reached its maximum length, we had high confidence in our estimates of minimum whisker age, but confidence surrounding maximum age was weak (Fig. 4). For instance, an 11 cm whisker could be no less than 90 d old, but maximum age could be up to 500 d. Moreover, longer whiskers had wider predicted age ranges compared to short whiskers (Fig. 4). The prediction of whisker age at a given length became much more powerful when only actively growing whiskers (i.e. not at L_∞) were included in the analysis (Fig. 4b). For example, a 10 cm whisker whose asymptotic length is >12.5 cm would still be in its rapid growth phase, so the predicted age range would be tighter than a 10 cm whisker at its asymptotic length (Fig. 4). Many of the 95% confidence intervals spanned a range of 40 to 100 d, which indicates that whisker age could be accurately predicted to 1–3 mo.
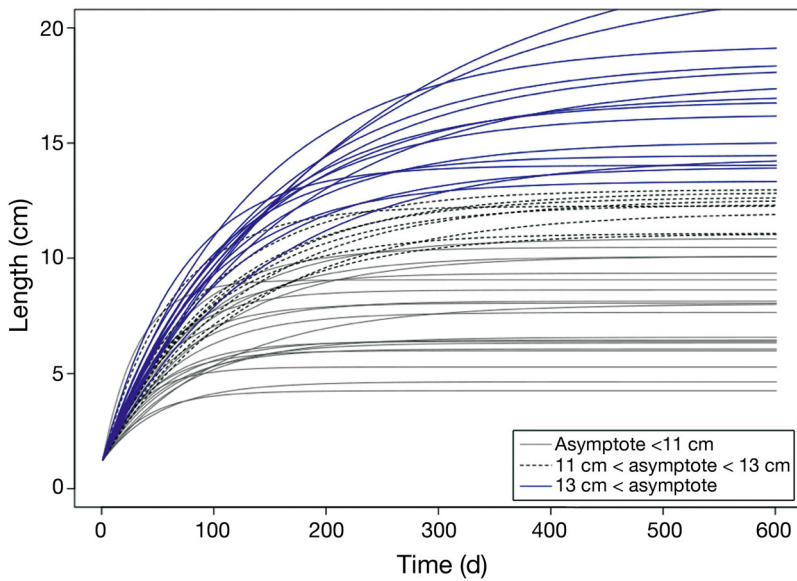
Fig. 3. *Mirounga angustirostris*. Growth trajectory of all whiskers of the captive elephant seal, showing high inter-whisker variation in curvature constant (K) and asymptotic whisker length (L_∞) values. Coloring identifies whiskers with various ranges of asymptotic lengths

whisker did not align with the other whiskers until dates were assigned to each sample. When stable isotope ratios were aligned based on whisker length, the $\delta^{15}N$ peaks of all whiskers (indicative of fasting by the wild seals) occurred over a range of 3.0 cm from the whisker tip. Based on the average curvature constant K from the captive seal's whiskers ($K = 0.0132$), the sections of whiskers where peaks occur represent a minimum temporal window of 83.2 d (Fig. 6a). After the whiskers were assigned timestamps using the average K from the captive seal's whiskers, the $\delta^{15}N$ peaks only ranged 14.0 d between animals (Fig. 6b). In 2 seals, the fasting peak in $\delta^{15}N$ coincided with haul-out; in the other 2, the fasting peak appeared just prior to haul-out (Fig. 6b). The temporal variation in $\delta^{15}N$ maxima likely results from uncertainty surrounding the amount of time those

Whisker bed anatomy

Maximum whisker length increased linearly with column position from the midline extending laterally (Fig. 5a). In contrast, whisker L_∞ increased across the first 5 descending rows, then decreased across the last 2 (Fig. 5a). The $L_\infty \approx$ column + row + row^2 model could be used to predict maximum whisker length for each row and column using:

$$L_\infty = 8.53 - 1.96y + 2.06x - 0.56x^2 \qquad (7)$$

where $y = $ column $- 4$ and $x = $ row $- 4$ ($R^2 = 0.85$; Fig. 5b). The model with a row^2 term provided the best fit (AIC = 329.8). The subsequent inclusion of a column^2 term gave no improvement in the model fit (AIC = 330.7). In the free-ranging seals, visible whisker length also increased along rows in a predictable fashion, such that the effective length of the next more caudal row neighbor of any whisker was 1.34 ± 0.27 (mean ± SD) times longer.

Applications of whisker growth dynamics to dietary reconstruction of wild elephant seals

The whiskers had mean (±SD) $\delta^{15}N$ values of 14.94 (±0.31‰), with maximum observed $\delta^{15}N$ of 17.56‰. The 4 whiskers obtained from the free ranging seals had different total lengths, so the highest $\delta^{15}N$ of each
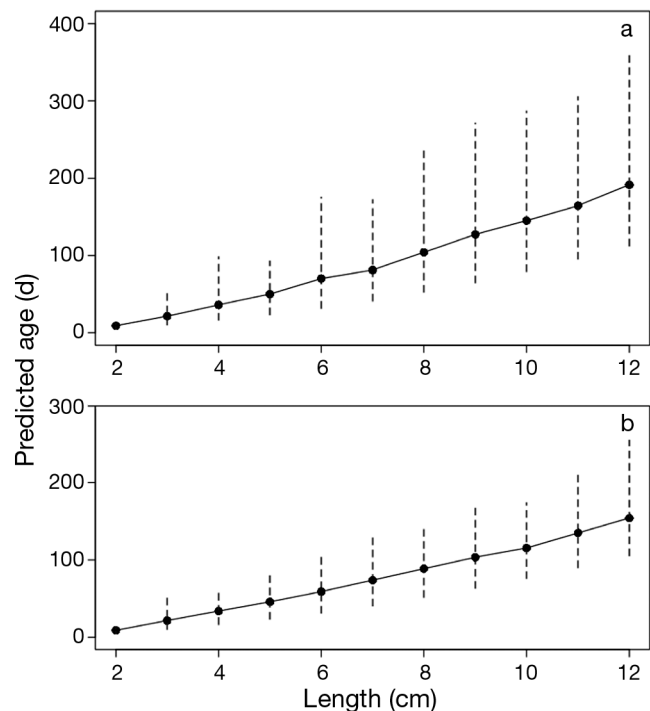

Fig. 4. *Mirounga angustirostris*. Predicted age as a function of size for (a) all whiskers and (b) 10 000 simulated whiskers at <75 % of their asymptotic length. Black line: mean prediction; error bars: 95 % confidence limits
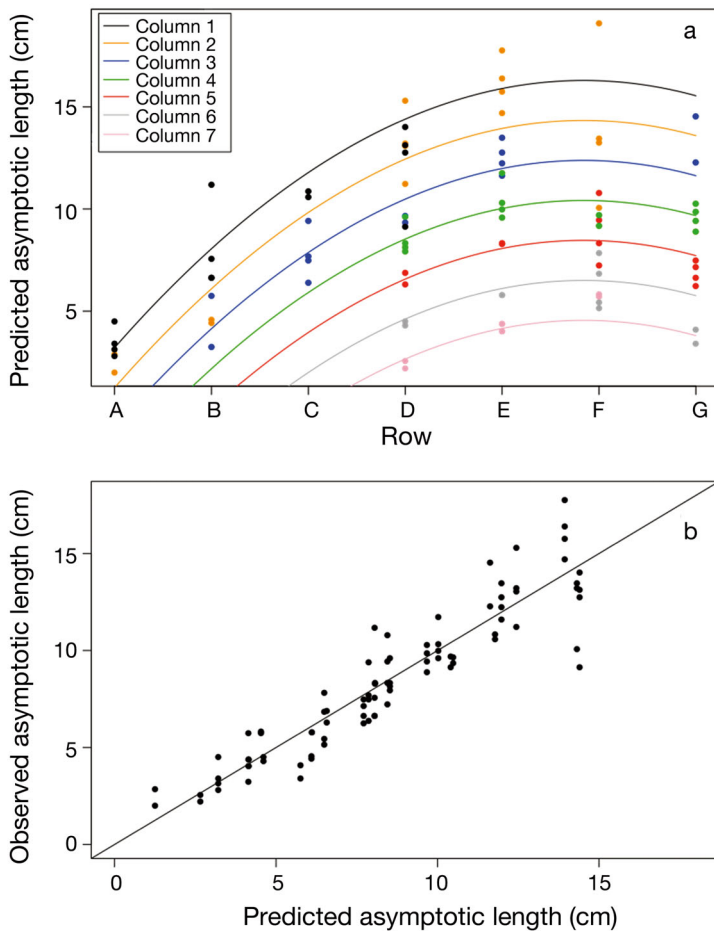
Fig. 5. (a) $L_\infty \approx$ column + row + row^2 model to predict maximum (i.e. asymptotic) length (L_∞) of whiskers in each row and column, and (b) variance in the relationship between observed and predicted L_∞. The measured length of each plucked whisker from 4 free-ranging adult female northern elephant seals fell within the 95% confidence intervals predicted for that follicle position by this multiple regression

whiskers were at L_∞ prior to extraction. These variations fell well within the 1 to 3 mo temporal range that can be used to predict whisker age with appropriate confidence (Fig. 4). Further, the growth model allowed us to predict the initial date of growth for each whisker, and the measured length of each plucked whisker fell within the 95% confidence intervals predicted for that follicle position by the multiple regression from the captive seal.

DISCUSSION

We developed and validated a broadly applicable approach for assigning time-stamps to stable isotope analysis data using quantitative whisker growth dynamics derived from a captive individual. We suc-

cessfully predicted and modeled von Bertalanffy growth parameters for individual whisker follicles, and identified the appropriate temporal resolution with which to estimate the age of a whisker with known length. Further, the growth rates calculated from the captive seal enabled us to assign stable isotope analysis data from the whiskers of free-ranging seals to appropriate time intervals. These are the highest resolution whisker growth data available for any mammal and the first in a northern elephant seal (Hobson & Sease 1998, Burton & Koch 1999, Clementz & Koch 2001, Aurioles et al. 2006).

Elephant seal whiskers exhibited a nonlinear, von Bertalanffy growth pattern consistent with that reported for other phocids, such as gray seals *Halichoerus grypus* (Greaves et al. 2004), harbor seals *Phoca vitulina* (Hirons et al. 2001) and leopard seals *Hydrurga leptonyx* (Hall-Aspland et al. 2005). The dynamics of von Bertalanffy growth allow individuals to maintain an intact whisker array by rapidly re-growing shed whiskers to a length effective for sensory function. This pattern of growth differs from the linear growth suggested for other amphibious mammals, including otariids (Steller sea lions *Eumetopias jubatus*; Hirons et al. 2001) and mustelids (southern sea otters *Enhydra lutris nereis*; Tyrrell et al. 2013). Our model focused on larger whiskers (>2 cm), because smaller, finer whiskers were difficult to measure using photogrammetry. We observed whiskers that were retained for well over a year; however, no follicle exhibited 2 full growth-to-shed cycles within the duration of our 670 d study. Some whiskers were still present after 500 d but none lasted all 670 d, suggesting that, in elephant seals, a single whisker lifespan can last for nearly 2 yr but not longer.

The amount of time represented by segments of each whisker differed vastly depending on the location on the whisker. For instance, a 0.5 cm segment at the base of a 10 cm whisker contained 52.5 d of foraging information, whereas the same size segment at the whisker tip represented only 5.2 d of foraging information. The absence of seasonal shedding patterns in our captive seal is consistent with the findings of Newland et al. (2011) for southern elephant seals *Mirounga leonina*, Greaves et al. (2004) for harbor seals, and Tyrrell et al. (2013) for sea otters. The ob-
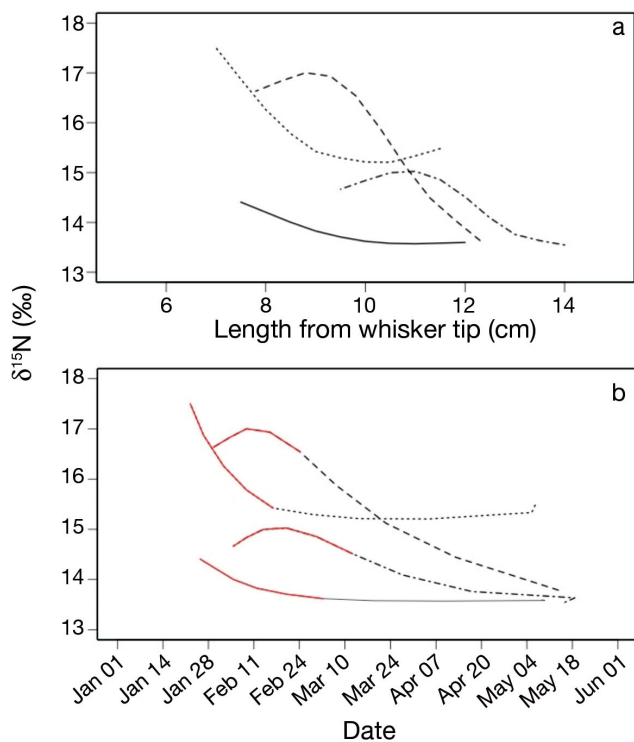
Fig. 6. *Mirounga angustirostris*. δ^{15}N values obtained for each 0.5 cm segment of vibrissae from 4 free-ranging adult female northern elephant seals. Each line represents 1 individual (identified by the same pattern in each panel) and is plotted as a function of: (a) length (in cm) from the tip of the vibrissa, such that the greatest lengths represent the most recently deposited tissues; and (b) calculated age of each analyzed whisker segment, using the average curvature constant from the captive seal's whiskers ($K = 0.0132$). Lines were smoothed using a Lowess algorithm on the raw stable isotope analysis data. Red sections of lines indicate the breeding haul-out period

served whisker shedding trends allow animals to maintain functional sensory systems year round.

For researchers interested in assigning age to whisker segments, we suggest plucking a whisker that has not reached asymptotic length (e.g. 75% of its asymptotic length). After a whisker reaches its maximum length, its age is difficult to determine because the whisker may have just reached this length (generally 100 to 150 d) or it could have reached L_∞ more than a year prior. Therefore, age predictions using whisker length will have higher accuracy if the sample whisker has not reached L_∞ and is still growing. Because no whisker within our sampled subset had an asymptote < 2 cm, the maximum age of a 2 cm whisker is constrained to less than 20 d; however, such short whiskers have turnover rates similar to plasma, serum, or red blood cells, and

as such, have limited advantage over other tissues commonly used for stable isotope analysis. For whiskers longer than 2 cm but not yet at L_∞, the range of potential whisker ages is narrower. To realistically apply parameter predictions from our captive study, it is necessary to determine which whisker on each row is not fully grown and should be preferentially extracted for stable isotope analysis. In the 4 free-ranging individuals we studied, visible whisker length increased along rows extending laterally, which is similar to the relationship reported by Brecht et al. (1997) for rats *Rattus norvegicus*. This relationship likely allows for the whisker array to conform to the contour of the muzzle when relaxed and subsequently form a flat plane when flexed forward (Towal et al. 2011). As a result, the expected difference in length between 2 adjacent whiskers can be used to preferentially extract whiskers that have not reached L_∞.

Our investigation provides a baseline model for serial growth studies of inert tissues using photogrammetry in vertebrates. Although we only followed whisker growth in a single individual living in captivity, this individual maintained a typical annual feeding/fasting cycle, and previous studies in harbor seals found no significant difference in growth rate between captive and free-ranging seals (Hirons et al. 2001, Greaves et al. 2004). While higher activity levels and extensive foraging migrations may lead to greater weathering of whisker tissue and potentially increased shedding rates, the growth parameters measured in the present study are likely specific to northern elephant seals, and applicable regardless of whether individuals are free-ranging or housed in captivity. Further, upon close examination of each whisker, we saw no evidence of abrasion during the study, and therefore posit that whisker abrasion did not affect whisker growth dynamics in the captive study.

Rather than extrapolating the elephant seal whisker growth dynamics to other species, we recommend conducting combined isotope and growth studies in those species where possible. Photogrammetry is an inexpensive method that requires no physical contact for captive, trained animals. Instead of logistical constraints such as those seen with other methods for estimating tissue growth, the number of growth intervals sampled in photogrammetry of captive individuals is only constrained by animal motivation and analysis time. To obtain adequate resolution of growth rates, we suggest that future whisker growth studies continue for a minimum of 1 yr, at a resolution of weekly or 2-weekly photo sessions.

Whiskers and other inert tissues record dietary information over relatively long periods as animals travel across extensive landscapes that are often completely inaccessible to researchers. Quantifying the growth rates of such archival tissues can further enhance the utility of stable isotope analysis by allowing researchers to assign relatively fine-scale temporal scales to their samples, so long as the resolution of the growth data respected. For instance, isotopic signatures from whiskers depict a large diversity of foraging strategies (Ben-David & Schell 2001, Cherel et al. 2009, Hückstädt et al. 2012b) and spatial distribution of prey items (Graham et al. 2010); when coupled with information about tissue growth, these isotope data will present a unique opportunity to reconstruct the seasonal habitats and diets of animals in scenarios that render other diet techniques impracticable.

LITERATURE CITED

Aurioles D, Koch PL, Le Boeuf BJ (2006) Differences in foraging location of Mexican and California elephant seals: evidence from stable isotopes in pups. Mar Mamm Sci 22:326–338

Bearhop S, Furness RW, Hilton GM, Votier SC, Waldron S (2003) A forensic approach to understanding diet and habitat use from stable isotope analysis of (avian) claw material. Funct Ecol 17:270–275

Ben-David M, Schell DM (2001) Mixing models in analyses of diet using multiple stable isotopes: a response. Oecologia 127:180–184

Bodey TW, Bearhop S, Roy SS, Newton J, McDonald RA (2010) Behavioural responses of invasive American mink *Neovison vison* to an eradication campaign, revealed by stable isotope analysis. J Appl Ecol 47:114–120

Bradshaw CJA, Hindell MA, Best NJ, Phillips KL, Wilson G, Nichols PD (2003) You are what you eat: describing the foraging ecology of southern elephant seals (*Mirounga leonina*) using blubber fatty acids. Proc R Soc B 270: 1283–1292

Bradshaw CJ, Hindell MA, Sumner MD, Michael KJ (2004) Loyalty pays: potential life history consequences of fidelity to marine foraging regions by southern elephant seals. Anim Behav 68:1349–1360

Brecht M, Preilowski B, Merzenich MM (1997) Functional architecture of the mystacial vibrissae. Behav Brain Res 84:81–97

Burton RK, Koch PL (1999) Isotopic tracking of foraging and long-distance migration in northeastern Pacific pinnipeds. Oecologia 119:578–585

Cherel Y, Kernaleguen L, Richard P, Guinet C (2009) Whisker isotopic signature depicts migration patterns and multiyear intra- and inter-individual foraging strategies in fur seals. Biol Lett 5:830–832

Clementz MT, Koch PL (2001) Differentiating aquatic mammal habitat and foraging ecology with stable isotopes in tooth enamel. Oecologia 129:461–472

Condit R, Le Boeuf BJ, Morris PA, Sylvan M (2007) Estimating population size in asynchronous aggregations: a bayesian approach and test with elephant seal censuses. Mar Mamm Sci 23:834–855

Connolly Sadou M, Beltran RS, Reichmuth C (2014) A calibration procedure for measuring pinniped vibrissae using photogrammetry. Aquat Mamm 40:213–218

Costa DP (2012) A bioenergetics approach to developing a population consequences of acoustic disturbance model. In: Popper AN, Hawkins A (eds) Advances in experimental medicine and biology. Springer, New York, NY, p 423–426

Dalerum F, Angerbjörn A (2005) Resolving temporal variation in vertebrate diets using naturally occurring stable isotopes. Oecologia 144:647–658

Gannes LZ, Del Rio CM, Koch P (1998) Natural abundance variations in stable isotopes and their potential uses in animal physiological ecology. Comp Biochem Physiol A Mol Integr Physiol 119:725–737

Graham BS, Koch PL, Newsome SD, McMahon KW, Aurioles D (2010) Using isoscapes to trace the movements and foraging behavior of top predators in oceanic ecosystems. In: West JB, Bowen GJ, Dawson TE, Tu KP (eds) Isoscapes: understanding movement, pattern, and process on earth through isotope mapping. Springer, Dordrecht, p 299–318

Greaves DK, Hammill MO, Eddington JD, Pettipas D, Schreer JF (2004) Growth rate and shedding of vibrissae in the gray seal, *Halichoerus grypus*: a cautionary note for stable isotope diet analysis. Mar Mamm Sci 20:296–304

Hall-Aspland SA, Rogers TL, Canfield RB (2005) Stable carbon and nitrogen isotope analysis reveals seasonal variation in the diet of leopard seals. Mar Ecol Prog Ser 305: 249–259

Hassrick J (2011) Demographic impacts on the foraging ecology of northern elephant seals. PhD dissertation,

University of California, Santa Cruz, CA

Hilborn R, Mangel M (1997) The ecological detective: confronting models with data. Princeton University Press, Princeton, NJ

Hirons AC, Schell DM, St Aubin DJ (2001) Growth rates of vibrissae of harbor seals (*Phoca vitulina*) and Steller sea lions (*Eumetopias jubatus*). Can J Zool 79:1053–1061

Hobson KA, Clark RG (1992) Assessing avian diets using stable isotopes II: factors influencing diet-tissue fractionation. Condor 94:189–197

Hobson KA, Sease JL (1998) Stable isotope analyses of tooth annuli reveal temporal dietary records: an example using Steller sea lions. Mar Mamm Sci 14:116–129

Hückstädt LA (2012) Dealing with a fast changing environment: the trophic ecology of the southern elephant seal (*Mirounga leonina*) and crabeater seal (*Lobodon carcinophaga*) in the western Antarctic Peninsula. PhD dissertation, University of California, Santa Cruz, CA

Hückstädt LA, Burns JM, Koch PL, McDonald BI, Crocker DE, Costa DP (2012a) Diet of a specialist in a changing environment: the crabeater seal along the western Antarctic Peninsula. Mar Ecol Prog Ser 455:287–301

Hückstädt LA, Koch PL, McDonald BI, Goebel ME, Crocker DE, Costa DP (2012b) Stable isotope analyses reveal individual variability in the trophic ecology of a top marine predator, the southern elephant seal. Oecologia 169: 395–406

Kuhn CE, Crocker DE, Tremblay Y, Costa DP (2009) Time to eat: measurements of feeding behaviour in a large marine predator, the northern elephant seal *Mirounga angustirostris.* J Anim Ecol 78:513–523

Le Boeuf BJ, Crocker DE, Costa DP, Blackwell SB, Webb PM, Houser DS (2000) Foraging ecology of northern elephant seals. Ecol Monogr 70:353–382

Lee SH, Schell DM, McDonald TL, Richardson WJ (2005) Regional and seasonal feeding by bowhead whales *Balaena mysticetus* as indicated by stable isotope ratios. Mar Ecol Prog Ser 285:271–287

Lee TN, Buck CL, Barnes BM, O'Brien DM (2012) A test of alternative models for increased tissue nitrogen isotope ratios during fasting in hibernating arctic ground squirrels. J Exp Biol 215:3354–3361

Lewis R, O'Connell TC, Lewis M, Campagna C, Hoelzel AR (2006) Sex-specific foraging strategies and resource partitioning in the southern elephant seal (*Mirounga leonina*). Proc R Soc B 273:2901–2907

Ling JK (1968) The skin and hair of the southern elephant seal *Mirounga leonina* (L.) III. Morphology of the adult integument. Aust J Zool 16:629–645

Logan JM, Lutcavage ME (2010) Stable isotope dynamics in elasmobranch fishes. Hydrobiologia 644:231–244

MacAvoy SE, Arneson LS, Bassett E (2006) Correlation of metabolism with tissue carbon and nitrogen turnover rate in small mammals. Oecologia 150:190–201

MacNeil MA, Skomal GB, Fisk AT (2005) Stable isotopes from multiple tissues reveal diet switching in sharks. Mar Ecol Prog Ser 302:199–206

Naito Y, Costa DP, Adachi T, Robinson PW, Fowler M, Takahashi A (2013) Unravelling the mysteries of a mesopelagic diet: a large apex predator specializes on small prey. Funct Ecol 27:710–717

Newland C, Field IC, Cherel Y, Guinet C, Bradshaw C, McMahon CR, Hindell MA (2011) Diet of juvenile southern elephant seals reappraised by stable isotopes in whiskers. Mar Ecol Prog Ser 424:247–258

Newsome SD, Tinker MT, Monson DH, Oftedal OT and others (2009) Using stable isotopes to investigate individual diet specialization in California sea otters (*Enhydra lutris nereis*). Ecology 90:961–974

Newsome SD, Clementz MT, Koch PL (2010) Using stable isotope biogeochemistry to study marine mammal ecology. Mar Mamm Sci 26:509–572

Newsome SD, Yeakel JD, Wheatley PV, Tinker MT (2012) Tools for quantifying isotopic niche space and dietary variation at the individual and population level. J Mammal 93:329–341

Ogden LJE, Hobson KA, Lank DB, Martínez del Rio C (2004) Blood isotopic (δ^{13}C and δ^{15}N) turnover and diet-tissue fractionation factors in captive dunlin (*Calidris alpina pacifica*). Auk 121:170–177

Oliver RF (1966) Whisker growth after removal of the dermal papilla and lengths of follicle in the hooded rat. J Embryol Exp Morphol 15:331–347

Robertson A, McDonald RA, Delahay RJ, Kelly SD, Bearhop S (2013) Whisker growth in wild Eurasian badgers *Meles meles*: implications for stable isotope and bait marking studies. Eur J Wildl Res 59:341–350

Robinson PW, Costa DP, Crocker DE, Gallo-Reynoso JP and others (2012) Foraging behavior and success of a mesopelagic predator in the northeast Pacific Ocean: insights from a data-rich species, the northern elephant seal. PLoS ONE 7:e36728

Sparre P, Venema SC (1999) Introduction to tropical fish stock assessment — Part 2: Exercises. FAO Fish Tech Pap 306/2 Revision 2. FAO, Rome

Thums M, Bradshaw CJA, Hindell MA (2011) In situ measures of foraging success and prey encounter reveal marine habitat-dependent search strategies. Ecology 92: 1258–1270

Towal RB, Quist BW, Gopal V, Solomon JH, Hartmann MJZ (2011) The morphology of the rat vibrissal array: a model for quantifying spatiotemporal patterns of whisker-object contact. PLoS Comput Biol 7:e1001120

Tyrrell LP, Newsome SD, Fogel ML, Viens M, Bowden R, Murray MJ (2013) Vibrissae growth rates and trophic discrimination factors in captive southern sea otters (*Enhydra lutris nereis*). J Mammal 94:331–338

Zhao L, Schell DM (2004) Stable isotope ratios in harbor seal *Phoca vitulina* vibrissae: effects of growth patterns on ecological records. Mar Ecol Prog Ser 281:267–273